Available online at www.sciencedirect.com
ScienceDirect
Acta Biomaterialia 4 (2008) 432–440
Acta BIOMATERIALIA
www.elsevier.com/locate/actabiomat

Effects of incorporation of hydroxyapatite and fluoroapatite nanobioceramics into conventional glass ionomer cements (GIC)

Alireza Moshaverinia [a], Sahar Ansari [a], Maryam Moshaverinia [b], Nima Roohpour [a], Jawwad A. Darr [c], Ihtesham Rehman [a,*]

[a] Department of Materials, Interdisciplinary Research Centre in Biomedical Materials, Queen Mary University of London, Mile End Road, London E1 4NS, UK
[b] Department of Oral Medicine, Mashhad Dental School, Mashhad University of Medical Sciences, P.O. Box 91735-984, Mashhad, Iran
[c] Department of Chemistry, University College London, Christopher Ingold Laboratories, 20 Gordon Street, London WC1H 0AJ, UK

Received 21 May 2007; received in revised form 4 July 2007; accepted 30 July 2007
Available online 25 August 2007

Abstract

Hydroxyapatite (HA) has excellent biological behavior, and its composition and crystal structure are similar to the apatite in the human dental structure and skeletal system; a number of researchers have attempted to evaluate the effect of the addition of HA powders to restorative dental materials. In this study, nanohydroxy and fluoroapatite were synthesized using an ethanol based sol–gel technique. The synthesized nanoceramic particles were incorporated into commercial glass ionomer powder (Fuji II GC) and were characterized using Fourier transform infrared and Raman spectroscopy, X-ray diffraction and scanning electron microscopy. Compressive, diametral tensile and biaxial flexural strengths of the modified glass ionomer cements were evaluated. The effect of nanohydroxyapatite and fluoroapatite on the bond strength of glass ionomer cement to dentin was also investigated. Results showed that after 1 and 7 days of setting, the nanohydroxyapatite/fluoroapatite added cements exhibited higher compressive strength (177–179 MPa), higher diametral tensile strength (19–20 MPa) and higher biaxial flexural strength (26–28 MPa) as compared with the control group (160 MPa in CS, 14 MPa in DTS and 18 MPa in biaxial flexural strength). The experimental cements also exhibited higher bond strength to dentin after 7 and 30 days of storage in distilled water. It was concluded that glass ionomer cements containing nanobioceramics are promising restorative dental materials with both improved mechanical properties and improved bond strength to dentin.

Keywords: Glass ionomer cement; Nanohydroxyapatie; Nanofluoroapatite; Sol–gel synthesis; Mechanical properties

1. Introduction

Glass ionomer cements (GIC) were invented by Wilson et al. at the Laboratory of the Government Chemist in 1969 [1,2]. These materials are water-based cements, and are also known as polyalkenoate cements [3]. They are based on the reaction between an alumino-silicate glass and polyacrylic acid, and cement formation arises from the acid–base reaction between the components [4,5]. The glass ionomer name is derived from the formulation of the glass powder and the ionomer that contains carboxylic acids. These cements are adhesive to tooth structure and translucent [6–8]. The matrix of the set cement is an inorganic–organic network with a highly cross-linked structure. The first glass ionomer cement (GIC) introduced had the acronym "ASPA", and comprised alumina-silicate glass as the powder and polyacrylic acid as the liquid. This product was first sold in Europe (De Trey Company and Amalgamated Dental Company) and later in the USA [9–11]. Glass ionomer cements have desirable properties, such as adhesion to moist tooth structure and an anticariogenic action (due to fluoride release). In addition, the coefficient of thermal expansion for glass ionomers is close to that of

* Corresponding author. Tel.: +44 20 7882 5502; fax: +44 20 8983 1799.
E-mail address: i.u.rehman@qmul.ac.uk (I. Rehman).

1742-7061/$ - see front matter
doi:10.1016/j.actbio.2007.07.011

tooth structure and they are biocompatible. Because of these unique properties, GICs are very useful and important as dental restorative materials [12–15]. In addition to their advantages, GICs suffer from the disadvantage of being brittle. Significant improvements have been made since the invention of GIC and are continuing to be made to enhance the physical properties of the cements. Although stronger and more aesthetic materials with improved handling characteristics are now available, lack of strength and toughness are still major problems [1–19].

Since hydroxyapatite (HA) has excellent biocompatible properties, and a composition and crystal structure similar to apatite in the human dental structure and skeletal system, a number of studies have tried to evaluate the effect of the addition of HA powders to restorative dental materials such as GICs [20–25]. Hydroxyapatite is a type of calcium phosphate, which is the main mineral component of the enamel of the tooth; it also comprises more than 60% of tooth dentine by weight. In addition, HA comprises the inorganic matrix of human bone in the form of phosphocalcic hydroxyapatite, which has the following formula $Ca_{10}(PO_4)_6(OH)_2$ and contains both phosphate and hydroxyl ions. The ability of HA to integrate with bone structures can help bonding between bone and implant structures and also support bone ingrowth without breaking down or dissolving [20,21].

GICs have been found to interact with HA via the carboxylate groups in the polyacid. Therefore, the incorporation of HA into GICs may not only improve the biocompatibility of GICs, but also have the potential of enhancing the mechanical properties. In addition, it has the ability to increase the bond strength to tooth structure due to its similar composition and structure to enamel and dentin. Lucas et al. [22,23] reported that the addition of the HA particles to the glass ionomer powder has the ability to increase the fracture toughness of the cement, which maintained long-term bond to dentin. Furthermore, they reported that the addition of HA did not hamper continued fluoride release and also maintained long-term bond strength to dentine. In addition, Gu et al. reported that GICs containing 4 wt.% HA particles exhibited enhanced mechanical properties in comparison with commercial GICs [24,25].

It is envisaged that the presence of HA and fluoroapatite (FA) nanoceramics in the GIC matrix have the ability to increase the mechanical and bond strength of the resulting material. Hence, the main aim of this study was to synthesize HA and FA nanoparticles and to assess the effect of their addition on the mechanical properties and bond strength to dentin of conventional GICs. Fuji II conventional GIC was used as the control group in this study due to its availability and popularity in dental communities; however, in next steps of these series of experiment the effects of addition of nanoceramics on properties of stronger and modern GICs such as Fuji IX and Ketac Molar will be investigated.

2. Materials and methods

2.1. Materials

The glass powders and all the liquids used in the experiments were of commercial grade, obtained from Fuji II (GC International, Tokyo, Japan). All the other chemicals in this study were of analytical grade and applied as received from Sigma–Aldrich Chemical Co. Calcium nitrate tetrahydrate [$Ca(NO_3)_2 \cdot 4H_2O$], $(NH_4)_2HPO_4$, ammonium fluoride (NH_4F), ethanol (C_2H_5OH) and ammonium hydroxide (NH_4OH) were used as obtained.

2.2. Synthesis of nanohydroxyapatite and nanofluoroapatite

Nanohydroxyapatite was produced by an ethanol-based sol–gel method similar to those of Kuriakose et al. [26] and Feng et al. [27].

Initially 6.6 g (50 mmol) of $(NH_4)_2HPO_4$ was dissolved in 50 ml of ethanol. In the second step, 19.702 g (84 mmol) of Ca $(NO_3)_2 \cdot 4H_2O$ was dissolved in 50 ml of ethanol in order to make a 0.5 M solution. This solution was added dropwise to the initial solution using a dropping funnel at the rate of 5 ml min^{-1}. The reaction was carried out at a constant temperature of 85 °C for 4 h. During the reaction, the pH of the solution was maintained at 10 by the dropwise addition of NH_4OH solution (up to a total amount of 5 ml).

For FA synthesis, the method described by Cavalli et al. [28] was adopted. In the experimental procedure initially 6.6 g (50 mmol) of $(NH_4)_2HPO_4$ was dissolved in 50 ml of ethanol, then 19.702 g (84 mmol) of $Ca(NO_3)_2 \cdot 4H_2O$ was dissolved in 50 ml of ethanol in order to make a 0.5 M solution. Subsequently, 0.62 g (16.7 mmol) of NH_4F with an appropriate molar ratio (Ca:P:F = 3:5:1) was added to the above solution as the source of fluoride ion. This solution was added dropwise to the initial solution using a dropping funnel at the rate of 5 ml min^{-1}. The reaction was carried out at a constant temperature of 85 °C for 4 h.

The nanopowders produced were dried using a freeze dryer (Wizard 2.0 SP Industries Co. The Virtis Company, NY). The powder samples were heat treated in a Carbolite® (Sheffield, UK) furnace. The samples were heated up to 400 °C at a rate of 10 °C min^{-1} and held at this temperature for 2 h, then heated at the same rate up to 800 °C and held for another 2 h at this temperature. Upon cooling, the powders were gently ground manually for 10 min using a mortar and pestle. The yields of each synthesis reaction were calculated and are tabulated in Table 1.

Table 1
Yield of synthesized HA and FA

Material	Yield (%)
Hydroxyapatite	78
Fluoroapatite	69

2.3. Characterization

2.3.1. Fourier transform infrared and Raman spectroscopy

Raman spectra of the nanobioceramic powders were obtained using a Nicolet Amelga XR dispersive Raman spectrophotometer. Sample was placed in a quartz tube and spectra were obtained in the range of 4000–400 cm^{-1}, averaging 256 scans at 2.0 s exposure time and 4 cm^{-1} resolution.

Fourier transform infrared (FTIR) spectra of the synthesized nano-HA and FA were obtained using a Nicolet 8700 FTIR spectrometer (Thermo Electron Corporation, UK) in conjunction with an MTEC photoacoustic sampling cell (PAS). The powder samples were put in the sample holder and the sampling chamber was purged with dry helium. Spectra were obtained in the mid-infrared region (4000–400 cm^{-1}) at 4 cm^{-1} resolution averaging 128 number of scans.

2.3.2. X-ray diffraction

The nanopowders produced in this study were analyzed with an X-ray diffraction (XRD) diffractometer (Siemens D5000 diffractometer) using Cu K radiation ($K_1 =$ 0.15406 nm; $K_2 = 0.1.5444$ nm). A powder sampling holder was used across the two range. The samples were set at a fixed position of 1° and the detector was scanned between 25° and 60° angles. A step size of 0.02° was used, with a step time of 2.5 s. Identification of phases was achieved by comparing the diffraction pattern obtained for the nanopowders and comparing their diffraction patterns with the standard cards on the ICDD-JCPDS database. Powdered samples were tested as produced and after calcination. Peak positions were determined using the XRD evaluation software EVA™ (Bruker-AXS, Germany).

2.3.3. Scanning electron microscopy and particle size analysis

Nano-HA and nano-FA powders were studied using a JEOL JSM 6300F high-resolution scanning electron microscope (SEM), which was operated at 15 keV. Samples were prepared by dispersing a thin layer of the powders on carbon coated copper grids. The mode of failure of dentin cement surfaces was also determined using SEM. Each specimen was coated with gold prior to analysis.

Particle sizes of the synthesized nanoceramics were measured using Zetasizer, nanoseries analyzer (ZS, Malvern Instruments Ltd. Worcestershire, UK) at 25 °C using a static light scattering method.

2.4. Formulation and evaluation of the modified glass ionomer cements

2.4.1. Specimen preparation

In order to prepare nano-HA- and nano-FA-containing glass powders, an appropriate amount (glass powder/HA and glass powder/FA ratio of 20:1 by wt.) of glass ionomer powder, and either nano-HA or nano-FA was weighed accurately and mixed gently by hand with a mortar and pestle for 20 min. The glass powder was Fuji II GIC (GC International, Tokyo, Japan) and a powder/liquid (P/L) ratio of 2.7/1 was used as recommended by the manufacturer. The GIC specimens were mixed and fabricated at room temperature according to the manufacturer's instructions.

Cylindrical specimens were prepared using PTFE cylindrical shaped molds 4 mm in diameter and 6 mm in height for compressive strength test and were cut to 2 mm thick cylinders for diametral tensile strength test. For the biaxial flexural strength test, PTFE cylindrical molds with 1 mm thickness and 10 mm diameter were used in order to prepare disc shaped samples with 10 mm diameter and 1 mm thickness. The molds were filled with the material and covered with PTFE tape and glass slides, flattened and gently pressed by hand in order to remove air bubbles from uncured cement paste. The specimens were removed from the molds after 30 min and conditioned in distilled water at 37 °C for 23.5 h and 7 days. Six specimens were made for each test. The different experimental groups of GICs and their abbreviations are tabulated in Table 2.

In order to measure the bond strength, 35 human extracted or impacted permanent third molars were stored and surface treated according to the procedures mentioned by Lucas et al. [22] (which complied with the ethical committee protocols of Mashhad Dental School, Iran). The treated teeth were then mounted in resin holders and both buccal and lingual surfaces of each tooth were trimmed with a low-speed trimmer. Subsequently, median grit silicon carbide papers (Grade P600, 1500) were used to obtain smooth dentin surfaces. Both the experimental group and the control group (Fuji II) cement samples were mixed according to the manufacturer's instructions and put into a material holder (3.0 mm diameter × 3.0 mm height). The samples were fitted by placing them in contact with the prepared dentin surfaces. The specimen assembly was then stored in 100% relative humidity at 37 °C for 1 h and then in distilled water for periods of 23 h, 7 days and 30 days.

2.4.2. Mechanical properties measurements

Mechanical tests were performed on a screw-driven mechanical testing machine (Model 4206, Instron Corp., Canton, MA) with a crosshead speed of 0.5 mm min^{-1}. The compressive strength was calculated from the relation-

Table 2
Compositions and the abbreviations used for various experimental glass ionomers

Group	Liquid composition	Powder composition
Fuji II	Polyacrylic acid copolymer	Strontium containing aluminum fluorosilicate glass
HM	Fuji II liquid	95 wt.% Fuji II glass, 5 wt.% HA nanopowder
FM	Fuji II liquid	95 wt.% Fuji II glass, 5 wt.% FA nanopowder

ship $CS = 4P/\pi d^2$, where P is the load (N) at the fracture point and d is the diameter (mm) of the cylindrical specimen. The diametral tensile strength (DTS) was determined according to the equation $DTS = 2P/\pi dt$, where P is the load at the fracture point, and d and t are the diameter and thickness (mm), respectively, of the specimen. For the biaxial flexural strength test, each specimen was placed on an 8 mm diameter annular knife-edged support ring (Instron Universal Testing machine), and the load to fracture at the rate of 0.5 mm min^{-1}, using a 3 mm diameter ballended indenter in a universal load testing machine, was recorded. Each specimen was tested at least six times. Biaxial flexural strengths were calculated from the following equation:

$$S = P/h^2(0.606 \ln a/h + 1.13)$$

where P is the load, h is the thickness of the sample and a is the diameter of the support ring. The constant of 1.13 is derived from the Poisson's ratio. From the previous studies of Akinmade et al. [29], the value of the Poisson's ratio was taken to be 0.27.

2.4.3. Bond strength measurement

After time intervals of 1 h, 1 day, 7 days and 30 days of storage in distilled water, a shear load was applied to the glass ionomer/dentin interface using a standard mechanical testing machine (Pand Industries Co., Iran) with a knife-edged rod at a crosshead speed of 0.5 mm min^{-1}. All the mechanical testing machines were calibrated prior to start the measurements. The shear force required to separate the cylinder from the dentine was recorded in Newtons and divided by the contact surface area, to determine the shear bond strength value in MPa. The debonded surfaces of the specimens were air dried and the mode of failure was determined using an SEM (JEOL JSM 6300F). The failure mode was classified according to one of following types: adhesive, cohesive in the cement, cohesive in dentin or mixed mode of failure.

The mean data obtained for mechanical and bond strength tests of specimens were analyzed by one-way analysis of variance with $\alpha = 0.05$.

3. Results

3.1. Characterization of synthesized bioceramics

The FTIR spectra of synthesized nano-HA and -FA powders are shown in Fig. 1a and b, and exhibited peaks at 3571, 1087, 1036, 936, 631, 601, 569 and 471 cm^{-1}, which were ascribed to the hydroxyl group of the HA, phosphate ν_3, phosphate ν_1, phosphate ν_4 and phosphate ν_2 vibrations, respectively. There were only two peaks at 875 and 1418 cm^{-1}, which belong to CO_3^{-2} ν_2 and ν_3 vibrations, respectively. It has been reported that carbonate ions, thought to originate from the CO_2 in air [28–30], can enter the structure of the HA. The OH peak centered at 3571 cm^{-1} disappeared in the FA spectrum. The peak at 631 cm^{-1} also disappeared, which confirmed the formation of FA. In the FA spectrum, the broad peak in the region of 1100–900 cm^{-1} is due to the phosphate modes, which increased in intensity after sintering. This can be attributed to the greater degree of crystallinity, which increases due to the sintering (Fig. 1a and b).

The peak assignments of the Raman and FTIR spectra of synthesized hydroxyl and FA powders confirmed that the final products were pure, and this correlated well with the previous studies by Cavalli et al. [28] and Rehman and Bonefield [30].

The XRD spectra of synthesized HA and FA nanoceramic powders are presented in Fig. 2. In all cases, the small size of the powders formed after freeze-drying led to broad peaks being observed in the XRD traces. After calcination of the powders in air at 800 °C for 2 h, the pattern obtained from the XRD traces were a good match to the pattern for phase pure HA and FA [JCPDS pattern 09-0432] (Fig. 2a and b). The HA and FA showed similar patterns and sharp peaks due to better crystallization at high temperatures. The peaks of HA at (2 1 1) and (1 1 2) merge due to fluorination [31]. The XRD patterns of the Fuji II glass ionomer sample, HA-added GIC and FA-added GIC after mixing with polyacid are shown in Fig. 3a–c, respectively. The Fuji II set cement sample (Fig. 3a) does not show any sharp peaks in the XRD analysis, indicating that it is a predominantly amorphous material, whereas in the XRD patterns of both the HA- and FA-added set GICs, peaks related to the crystalline apatite structure were observed between 20° and 35° (Fig. 3b and c). These results correlated well with those reported previously by Milne et al. [36].

SEM images of the sample powders are shown in Fig. 4. These images revealed that all the powders were in the nanosize range and granular in shape. Representative SEM micrographs of the dentin and glass debonded surfaces are shown in Fig. 5. All of the samples showed a cohesive mode of failure in the material. SEMs and the results from the particle size analyzer showed that the particle sizes of both the HA and the FA were approximately 100–200 nm.

3.2. Mechanical and bond strength properties

The results of 1 and 7 days of CS, DTS and BFS values of the nano-HA- and nano-FA-containing glass ionomers are shown in Fig. 6 and compared with values for Fuji II GIC as the control group. The results show that there is a significant difference between the CS, DTS and BFS values of the HA- and FA-containing GIC samples and the control group. Nano-HA-containing glass ionomer (HM), which was mixed with the liquid of Fuji II, exhibited higher mechanical strength values than the control group and the same trend was observed for the nano-FA-containing glass ionomer samples (FM). The mechanical results for the FA-added GIC are higher than those of the HA-added GIC after 7 days of storage in distilled water (Fig. 6).

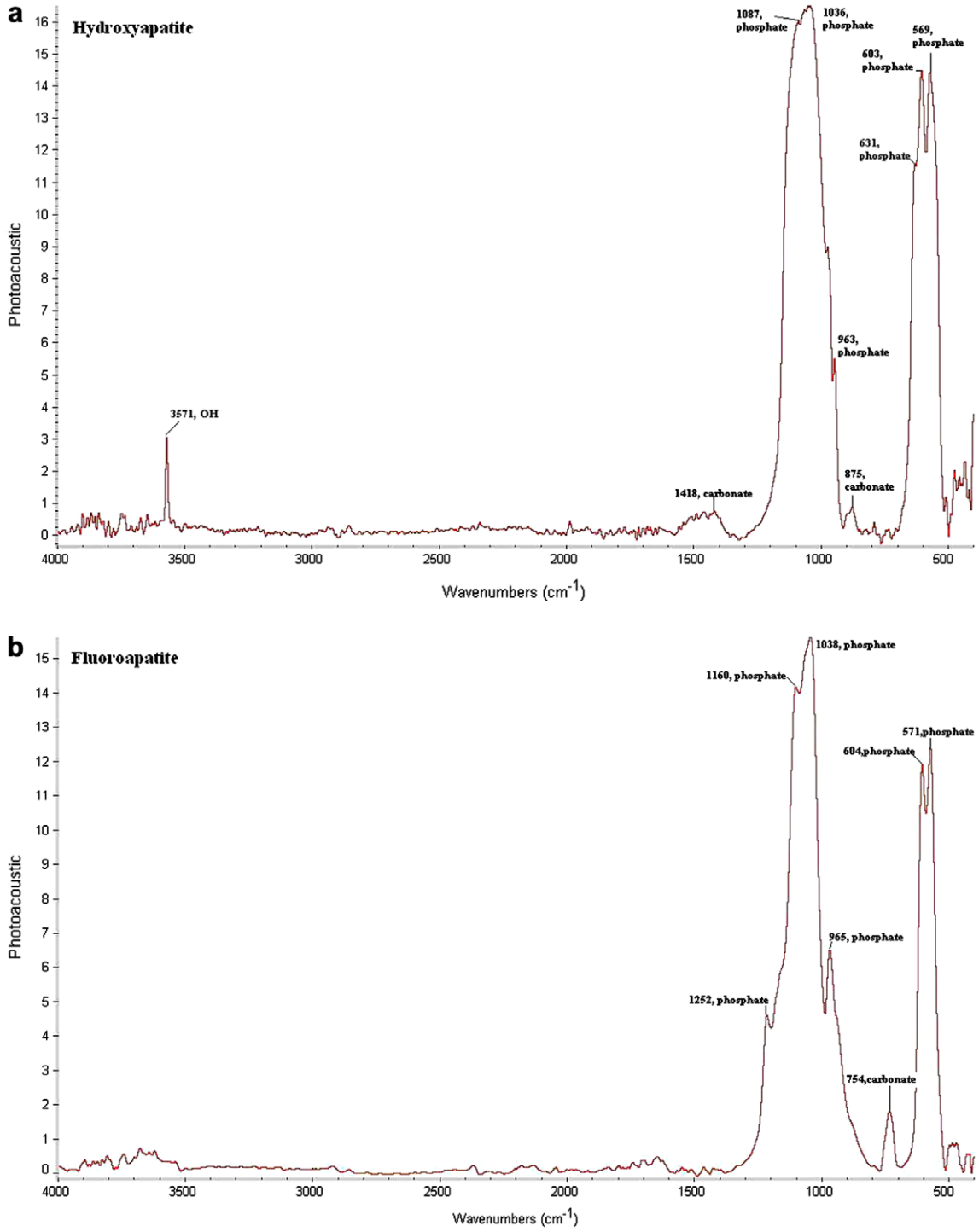

Fig. 1. FTIR spectra of the synthesized nanopowders of HA (a) and FA (b); note the disappearing of the peaks at 3571 and 631 cm^{-1} in the FA sample, confirming the formation of FA.

The bond strength values of the bioceramic-added GIC and the control group after 1 h, 24 h, 7 days and 30 days of storage in distilled water are shown in Fig. 7. The bond strengths of the FA-modified (8.4 ± 1.7 MPa, after 7 days) and HA-modified (8.2 ± 1.8 MPa, after 7 days) specimens were not significantly different after 7 days of storage in distilled water, while their results were higher than those of the control group (7.3 ± 1.5 MPa for GIC after 7 days). The highest values were related to the FA-added GIC samples.

4. Discussion

The resulting peaks in the FTIR and Raman spectra of HA nanoparticles were in agreement with the previous studies by Rehamn et al. and Philips et al. [30] and [31]

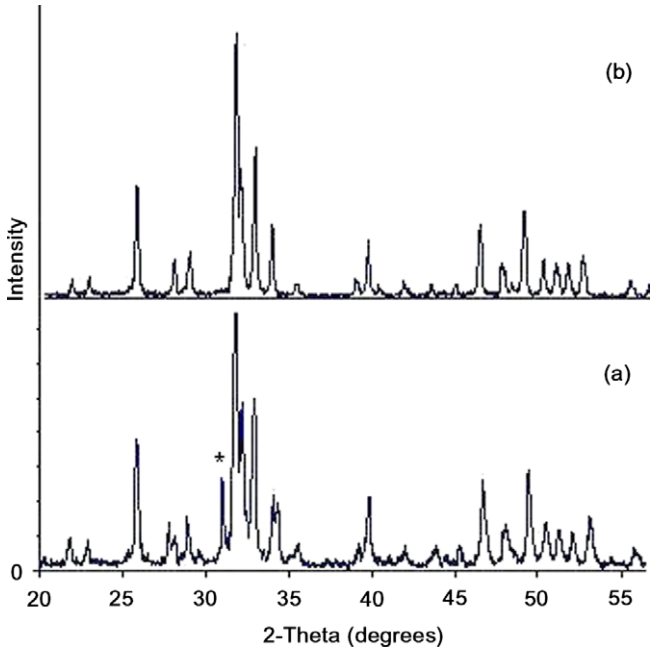

Fig. 2. XRD traces of HA (a) and FA (b) nanoceramic powders after calcination in air at 800 °C for 2 h.

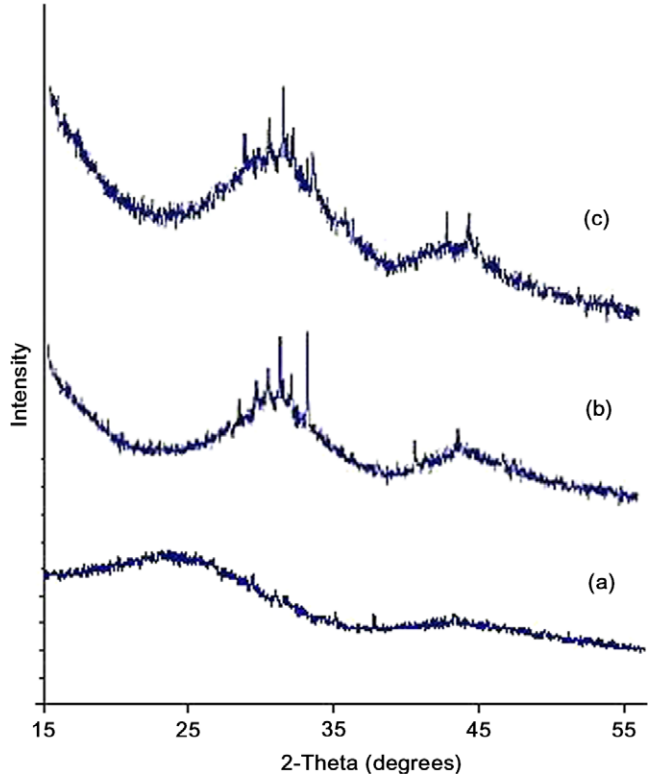

Fig. 3. XRD traces of Fuji II GIC (a), HA-added GIC (b) and FA-added GIC (c) after mixing with polyacrylic acid.

respectively, Nikčević et al. [32] and Redey et al. [33]. The OH peak disappeared in the FA spectra and a broad peak in the 1100–900 cm^{-1} regions was observed which correlates with a former study by Wei et al. [34]. In addition,

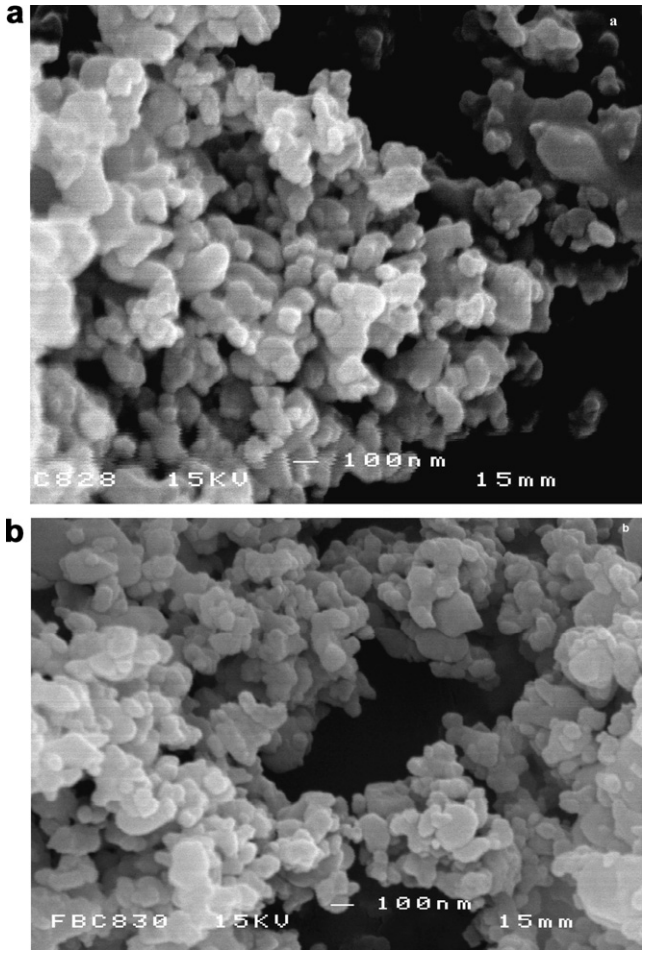

Fig. 4. SEM of HA (a) and FA (b) nanopowders (40,000×).

the XRD results showed that the synthesized bioceramics had low degrees of impurity, high degrees of crystallinity and structures correlated with hydroxyl and FA chemical compositions [35]. This observation was in agreement with the fact that fluorine addition tends to decrease the lattice parameter *a*, but not obviously affect the lattice parameter *c*. It can be seen in Fig. 1b that the peaks of the FA are sharper than those of pure HA. Thus, the incorporation of fluorine into the HA matrix increased the crystallinity of the final crystals. The increased crystallinity corresponded to the increased chemical stability of the FA bioceramic nanopowders [31,35,36].

Mechanical tests results showed that all the GICs became stronger as they matured after 1 and 7 days of storage in distilled water at 37 °C. Previous studies have shown that nano-HA is a promising additive to glass ionomer powder; Yap et al. [37] reported that Fuji IX glass ionomer with 4 wt.% HA in its composition had higher compressive and diametral tensile strength (CS = 177.27 MPa, DTS = 13.94 MPa) than non-reinforced commercial Fuji IX (CS = 135 MPa, DTS = 12.07 MPa). In this study, nanoparticles (100–200 nm) of both HA and FA were added to glass ionomer powder (5 wt.%) and the mechanical test results showed that both glass powders had higher strength

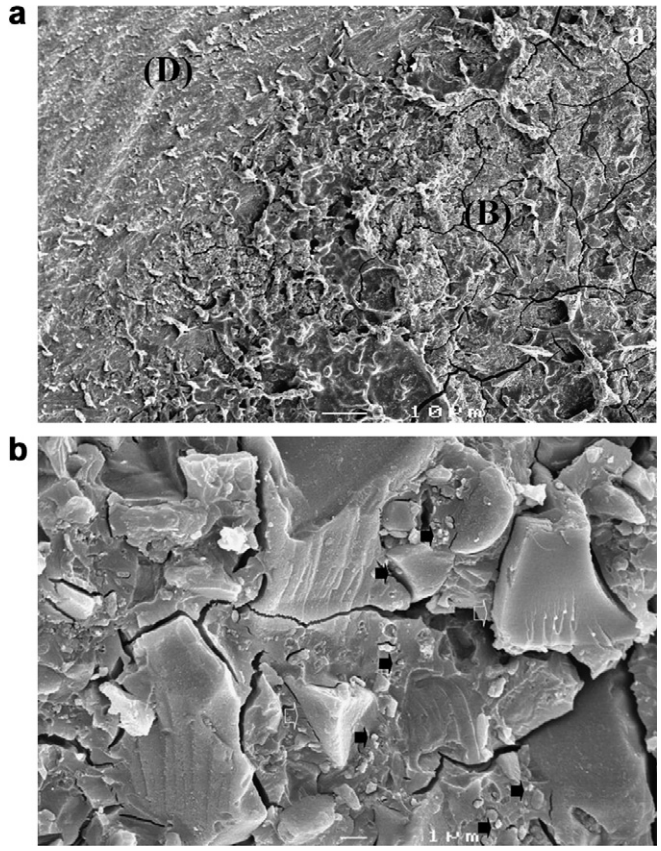

Fig. 5. SEM of a fracture surface from cohesively failed FA-added GIC as an example of dentin–GIC debonding. (a) Fractured surface showing retained GIC bulk (B) and dentin structure (D) (1500×); (b) GIC matrix overlying the dentin surface. Note the presence of exposed tiny glass cores (white arrows) and nanoceramic particles (black arrows) (5000×).

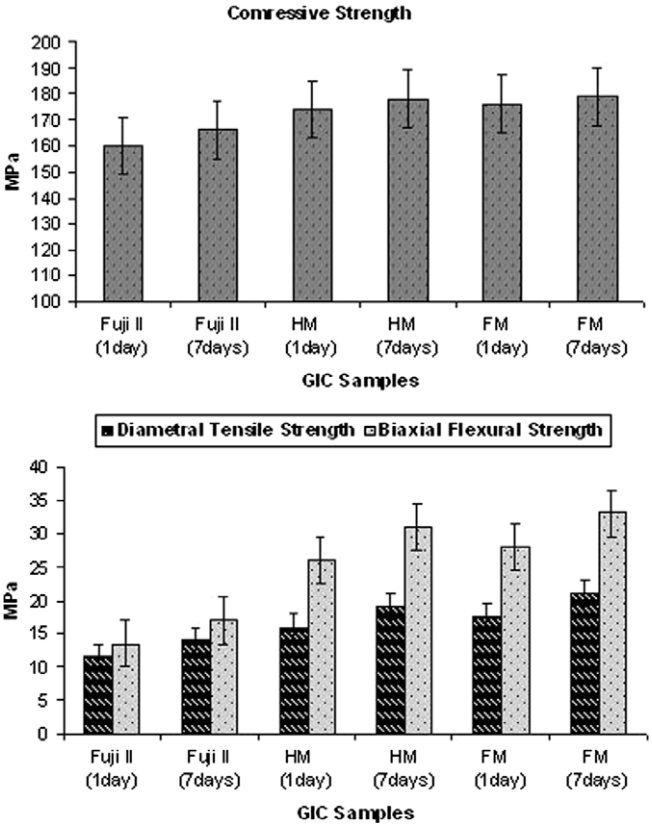

Fig. 6. Mechanical test (compressive, diametral tensile and biaxial flexural strength) results of the GIC samples after 1 and 7 days of storage in distilled water at 37 °C.

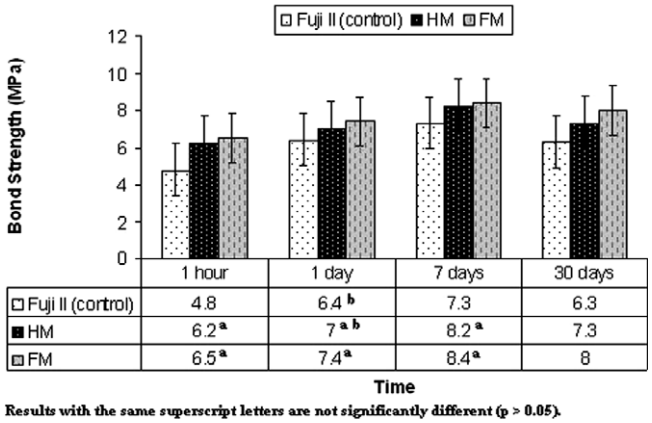

	1 hour	1 day	7 days	30 days
Fuji II (control)	4.8	6.4 [b]	7.3	6.3
HM	6.2 [a]	7 [a,b]	8.2 [a]	7.3
FM	6.5 [a]	7.4 [a]	8.4 [a]	8

Results with the same superscript letters are not significantly different ($p > 0.05$).

Fig. 7. Bond strength to dentin (MPa); comparison between the experimental GICs and Fuji II ($n = 5$).

compared with the Fuji II commercial GICs. Nano-FA/ionomers had higher values for CS, DTS and BFS (179, 23 and 33 MPa, respectively) compared with HA/ionomer (178, 19 and 31 MPa, respectively), which can be related to the stability of FA and its lower dissolution rate in distilled water compared with that of nano-HA. A more than 14% increase in CS was observed and the values for diametral tensile strength increased up to 70%, while the values for biaxial flexural strength increased to more than 90%. This suggested that these additives have an affect on both the setting reaction mechanism and the degree of polysalt bridge formation of the glass ionomer, which improve the mechanical properties of the final set cement. Hydroxyapatite and to some extent FA nanoceramics are soluble in acidic solutions; as a result, calcium ions can be extracted from the surface of HA and FA after mixing the powder with a polyacid. There might be higher degrees of acid–base reaction within the structure of the setting cement due to presence of HA and FA, which lead to stronger cements [38]. Both nano-HA and FA are involved in the acid–base reaction of the GIC and react with inorganic/organic components of the GIC network via their phosphate and calcium ions. Thus, by incorporation of FA and HA into a GIC powder composition, after H^+ attack the ceramic particles, there would be more Ca^{2+} ion available for cement formation, polysalt bridge formation and cross-linking, all of which reinforce the GIC matrix. Both modified glass powders exhibited higher values in mechanical tests in comparison with Fuji II GIC samples. The possibility of the formation of hydrogen bonds may be greater because of the presence of additional hydroxyl, phosphate and fluoride ions in the matrix. Without doubt, stronger bonds between the organic and inorganic network of the

set cement lead to higher mechanical strength of the final set cement.

The cohesive fracture of a glass ionomer–dentin surface has been reported in the literature previously [22,39]. In this study, scanning electron micrographs of the fractured surface of the dentin of control GIC showed a retained GIC bulk and a thin cement matrix. In Fig. 5a, the fractured side of dentin after debonding from the FA-added GIC sample is shown as an example of the failure mode observed in this series of experiments. However, the SEM of HA- and FA-added samples showed cohesive failure with a thicker cement layer in comparison with the control group. These results agree well with previously reported studies in the literature, which have reported that the strength of the cement–tooth bond is higher than the inherent strength of the material [22,39]. The fractured HA- and FA-added cements revealed the presence of a glass core and HA and FA nanoparticles, respectively, embedded on the surface even in the thin matrix area. It is also interesting to note that the addition of HA and FA nanoparticles may result in a strengthened matrix and subsequently better bonding to the bulk of the glass and matrix. However, due to debonding, some cracking appeared on the surface of the remaining GIC bulk on the dentin surface, which can be observed in the SEM photographs presented in Fig. 5a and b.

The bond strength results correlate well with the results reported previously by Wilson and McLean [2], Arora and Deshpande [40] and Lucas et al. [22]. Wilson and McLean [2] reported that the bond strength of Fuji II GIC to tooth structure is about 5–6 MPa. Lucas et al. [22] also reported that HA-added conventional GIC and Fuji IX exhibited bond strength values of 5.3 and 5.2 MPa, respectively. The bond strength results showed that there was no significant difference between the bond strength of FA-added GIC (8.4 ± 1.7 MPa) and HA-added GIC (8.2 ± 1.8 MPa) after 7 days of storage in distilled water, while after 30 days, due to the lower rates of dissolution of FA particles in comparison with HA particles, a considerable difference between the bond strength values of the FA- and HA-added GIC samples was observed (8.0 MPa for HA-added GIC and 7.3 MPa for FA-added GIC, respectively). Due to the lower degrees of solubility of FA in distilled water in comparison with HA, the bond strength values and mechanical test results of the samples containing FA nanoparticles were higher than the values of samples containing HA nanoparticles after 7 and 30 days of storage in distilled water. In addition, due to the presence of phosphate, hydroxyl and fluoride ions in the intermediate layer between the cement and the tooth structure, there is a greater possibility of the formation of ionic and hydrogen bonds between the GIC and tooth substrate, which is the main cause of the increased bond strength values for the HA- and FA-added GICs in comparison with the control group. This phenomenon can be attributed to the greater availability of bonds between the tooth structure and the modified GIC samples. Regarding the small sizes of the nanoceramics incorporated into the glass powder of GIC, the resulting experimental glasses had wider ranges of particle size distribution (the average particle size of the glass ionomer particles was around 5–10 μm in this study), which resulted in higher mechanical values. Consequently, these groups can occupy the empty spaces between the glass ionomer glass particles and act as a reinforcing material in the composition of the GICs. Finally, the presence of fluoride in the fluoride-substituted apatite has the potential to increase the amount of fluoride release from the set GICs, and this will be investigated further in future.

5. Conclusion

The addition of nano-HA and FA synthesized into Fuji II commercial GIC enhanced the mechanical properties (compressive, diametral tensile and biaxial flexural strength) of the resulting cements and their bond strengths to dentin. These bioceramics are therefore considered promising additives for glass ionomer restorative dental materials. However, possibly due to the lower solubility rate of FA, the FA-containing samples showed higher values after 7 and 30 days for both the mechanical and bonding tests in comparison with HA-added GIC samples.

Acknowledgement

A.M. greatly acknowledges the expert advice of Mr. R.W. Billington.

References

[1] Wilson AD, Kent BE. The glass ionomer cement, a new transluscent dental filling material. J Appl Chem Biotechnol 1971;21:313.
[2] Wilson AD, McLean JW. Glass-ionomer cement. second ed. Chicago, IL: Quintessence Books; 1988.
[3] Crisp S, Ferner AJ, Lewis BG, Wilson AD. Properties of improved glass-ionomer cement formulations. J Dent 1975;3:125–30.
[4] McLean JW, Gasser O. Glass-cermet cements. Quint Int 1985;16:333–43.
[5] Wilson AD, Nicholson JW. Acid–base cements: their biomedical and industrial applications. Cambridge: Cambridge University Press; 1993.
[6] Davidson CL. Advances in glass ionomer cements. Chicago, IL: Quintessence Publishing Co.; 1993.
[7] Smith DC. Development of glass ionomer cement systems. Biomaterials 1998;125:381–94.
[8] McLean JW, Nicholson JW, Wilson AD. Proposed nomenclature for glass ionomer dental cements and related materials. Quintessence Int 1994;25:587–9.
[9] Wilson AD, Kent BE. A new translucent cement for dentistry, the glass ionomer cement. Brit Dent J 1972;132:133–5.
[10] Powers JM, Sakaguchi RL. Craig's restorative dental materials. 12th ed. London: Elsevier; 2006.
[11] Wilson AD. Resin-modified glass ionomer cements. Inter J Prosth 1989;2:438–46.
[12] Walls AW. Glass polyalkenoate (glass ionomer) cements. J Dent 1986;14:231–46.
[13] Anusavice KJ. Philips science of dental materials. 11th ed. Philadelphia, PA: Saunders; 2003.

[14] Smith DC. Polyacrylic acid-based cements – adhesion to enamel and dentine. Oper Dent 1999;5:177–83.
[15] Kent BE, Lewis BG, Wilson AD. Glass-ionomer cement formulations: I. The preparation of novel fluoroaluminosilicate glasses high in fluorine. J Dent Res 1979;58:1607–19.
[16] Nicholson JW. Chemistry of glass-ionomer cements: a review. Biomaterials 1998;6:485–94.
[17] Crisp S, Lewis BG, Wilson AD. Gelation of polyacrylic acid aqueous solutions and the measurement of viscosity. J Dent Res 1975;54:1173–5.
[18] McLean JW, Powis DR, Prosser HJ, Wilson AD. The use of glass ionomer cements in bonding composite resins to dentine. Br Dent J 1985;158:410–4.
[19] Culbertson BM. Glass-ionomer restorative materials. Prog Polym Sci 2001;26:577–604.
[20] Elliott JC. Structure and chemistry of the apatites and other calcium orthophosphates. London: Elsevier; 1994.
[21] LeGeros RZ. Calcium phosphates in demineralization and remineralization processes. J Clin Dent 1999;10:65–73.
[22] Lucas ME, Arita K, Nishino M. Toughness, bonding and fluoride-release properties of hydroxyapatite-added glass ionomer cement. Biomaterials 2003;24:3787–94.
[23] Lucas ME, Arita K, Nishino M. Strengthening a conventional glass ionomer cement using hydroxyapatite. J Dent Res 2002;81:36.
[24] Gu YW, Yap AUJ, Cheang P, Khor KA. Effects of incorporation of HA/ZrO(2) into glass ionomer cement (GIC). Biomaterials 2005; 26:713–20.
[25] Gu YW, Yap AUJ, Cheang P, Khor KA. Development of zirconia–glass ionomer cement composites. J Non-Cryst Solids 2005;351: 508–14.
[26] Kuriakose T, Kalkura N, Palanichamy M, Arivuoli D, Bocelli G, Betzel C. Synthesis of stoichiometric nano crystalline hydroxyapatite by ethanol-based sol–gel technique at low temperature. J Crys Growth 2004;263:517–23.
[27] Feng W, Mu-sen L, Yu-peng L, Yong Q. A simple sol–gel technique for preparing hydroxyapatite nanopowders. Mater Lett 2005;59: 916–20.
[28] Cavalli M, Gnappi G, Montenero A, Fini M. Hydroxy- and fluorapatite films on Ti alloy substrates: sol–gel preparation and characterization. J Mater Sci 2001;36:3253–60.
[29] Aknimade AO, Nicholson JW. Poisson's ratio of glass polyalkenoate cements determined by an ultrasonic methods. J Mater Sci: Mater Med 1995;6:1573–4838.
[30] Rehman I, Bonfield W. Characterization of hydroxyapatite and carbonated apatite by photo acoustic FTIR spectroscopy. J Mater Sci: Mater Med 1997;8:1–4.
[31] Philips MJ. Chemical coupling of biocomposites: surface modification of bioceramics creating chemically bound polymer composites with potential osteological applications. PhD thesis, Queen Mary, University of London; 2005.
[32] Nikčević I, Jokanović V, Mitrić M, Nedić Z, Makovec D, Uskoković D. Mechanochemical synthesis of nanostructured fluorapatite/fluorhydroxyapatite and carbonated fluorapatite/fluorhydroxyapatite. J Sol Sta Chem 2004;17:2565–74.
[33] Redey S, Nardin M, Bernache-Assolant D, Rey C, Delannoy P, Sedel L, Marie P. Behavior of human osteoblastic cells on stoichiometric hydroxyapatite and type A carbonate apatite: role of surface energy. J Biomed Mater Res 2000;50:353–9.
[34] Wei W, Evans JH, Bostrom T, Grondahl L. Synthesis and characterization of hydroxyapatite, fluoride-substituted hydroxyapatite and fluorapatite. J Mater Sci 2003;14:311–20.
[35] Chen Y, Miao X. Thermal and chemical stability of fluorohydroxyapatite ceramics with different fluorine contents. Biomaterials 2005;11:1205–10.
[36] Milne KA, Calos NJ, O'Donnell JH, Kennard CHL, Vega S, Marks D. Glass-ionomer dental restorative. Part I: A structural study. J Mater Sci: Mater Med 1997;8:349–56.
[37] Yap AUJ, Pek YS, Kumar RA, Cheang P, Khor KA. Experimental studies on a new bioactive material: HA ionomer cements. Biomaterials 2002;23:955–62.
[38] Aoki H. Science and medical applications of hydroxyapatite. Tokyo: Takayama Press System Centre Co.; 1991.
[39] Fruits TJ, Duncanson MG, Miller RC. Bond strengths of fluoride-releasing restorative materials. Am J Dent 1996;9:219–22.
[40] Arora R, Deshpande SD. Shear bond strength of resin-modified restorative glass ionomer cements to dentin – an in vitro study. J Indian Soc Pedod Prev Dent 1998;16:130–3.